



**HAL**  
open science

# CHAOS IN A THREE-DIMENSIONAL VOLTERRA-GAUSE MODEL OF PREDATOR-PREY TYPE

Jean-Marc Ginoux, Bruno Rossetto, Jean-Louis Jamet

► **To cite this version:**

Jean-Marc Ginoux, Bruno Rossetto, Jean-Louis Jamet. CHAOS IN A THREE-DIMENSIONAL VOLTERRA-GAUSE MODEL OF PREDATOR-PREY TYPE. International journal of bifurcation and chaos in applied sciences and engineering , 2005, 15 (5), pp.1689. 10.1142/S0218127405012934 . hal-01026173

**HAL Id: hal-01026173**

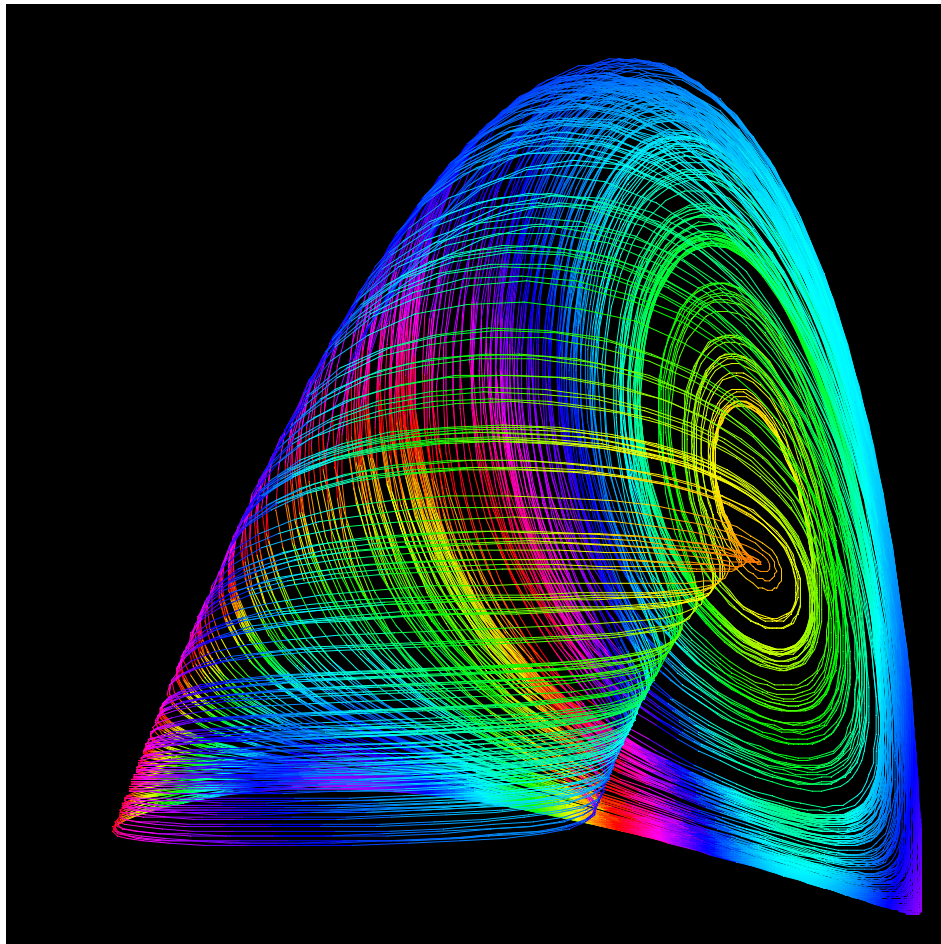
**<https://univ-tln.hal.science/hal-01026173>**

Submitted on 21 Jul 2014

**HAL** is a multi-disciplinary open access archive for the deposit and dissemination of scientific research documents, whether they are published or not. The documents may come from teaching and research institutions in France or abroad, or from public or private research centers.

L'archive ouverte pluridisciplinaire **HAL**, est destinée au dépôt et à la diffusion de documents scientifiques de niveau recherche, publiés ou non, émanant des établissements d'enseignement et de recherche français ou étrangers, des laboratoires publics ou privés.

# CHAOS IN A THREE-DIMENSIONAL VOLTERRA-GAUSE MODEL OF PREDATOR-PREY TYPE



JEAN-MARC GINOUX, BRUNO ROSSETTO AND JEAN-LOUIS JAMET

*PROTEE Laboratory, University of South Toulon Var, B.P. 20132,  
83957, LA GARDE Cedex, France*

E-mail: [ginoux@univ-tln.fr](mailto:ginoux@univ-tln.fr), [rossetto@univ-tln.fr](mailto:rossetto@univ-tln.fr), [jamet@univ-tln.fr](mailto:jamet@univ-tln.fr)

# CHAOS IN A THREE-DIMENSIONAL VOLTERRA-GAUSE MODEL OF PREDATOR-PREY TYPE

JEAN-MARC GINOUX, BRUNO ROSSETTO AND JEAN-LOUIS JAMET

*PROTEE Laboratory, University of South Toulon Var, B.P. 20132,  
83957, LA GARDE Cedex, France*

E-mail: [ginoux@univ-tln.fr](mailto:ginoux@univ-tln.fr), [rossetto@univ-tln.fr](mailto:rossetto@univ-tln.fr), [jamet@univ-tln.fr](mailto:jamet@univ-tln.fr)

## *Abstract*

*The aim of this paper is to present results concerning a three-dimensional model including a prey, a predator and top-predator, which we have named the Volterra-Gause because it combines the original model of V. Volterra incorporating a logistic limitation of the P.F. Verhulst type on growth of the prey and a limitation of the G.F. Gause type on the intensity of predation of the predator on the prey and of the top-predator on the predator. This study highlights that this model has several Hopf bifurcations and a period doubling cascade generating a snail shell-shaped chaotic attractor.*

*With the aim of facilitating the choice of the simplest and most consistent model a comparison is established between this model and the so-called Rosenzweig - MacArthur and Hastings-Powell models. Many resemblances and differences are highlighted and could be used by the modellers.*

*The exact values of the parameters of the Hopf bifurcation are provided for each model as well as the values of the parameters making it possible to carry out the transition from a typical phase portrait characterising one model to another (Rosenzweig-MacArthur to Hastings-Powell and vice versa).*

*The equations of the Volterra-Gause model cannot be derived from those of the other models, but this study shows similarities between the three models.*

*In cases in which the top-predator has no effect on the predator and consequently on the prey, the models can be reduced to two dimensions.*

*Under certain conditions, these models present slow-fast dynamics and their attractors are lying on a slow manifold surface, the equation of which is given.*

*Keywords: Chaos; strange attractors; predator-prey models; slow-fast dynamics.*

---

# 1. Introduction

The paper is organized as follows. In the following section we will study a three-dimensional Volterra-Gause\* model in the most general case. The stability of the fixed points according to the works of Freedman and Waltman [1977] and the occurrence of Hopf bifurcation in this model are examined. This analysis shows that such a bifurcation exists in the  $xy$  plane and is possible apart from the  $xy$  plane.

Then, the study of the Volterra-Gause model for particular values of parameters ( $k = p = 1/2$ ), checking for the existence of bifurcations in the  $xy$  plane and apart from the  $xy$  plane and determining the values of the bifurcation parameters.

Dynamic analysis of this particular case demonstrate the existence of a chaotic attractor in the shape of a snail shell.

The bifurcation diagrams indicates the existence of a period doubling cascade leading to chaos.

The section ends with another particularly dynamical aspect which is, that under certain conditions, this model presents slow-fast dynamics.

So, according to the works of Ramdani *et al.*, [2000], we give the slow manifold equation of the surface on which trajectories of the attractor are lying on.

The aim of the last section is to compare the most used predator – prey models.

We begin by summarising the general properties of the Rosenzweig-MacArthur [1963] and Hastings-Powell [1991] models, including the stability of fixed points, the value of the Hopf bifurcation parameter and the equation of the slow manifold surface.

In the Hastings-Powell [1991] model, we show, against expectations, that some of the trajectories of the so-called “teacup” also lie on a surface.

Similarities in behaviour between these three models are highlighted:

the nature and number of fixed points, type of bifurcation, shape of the attractor.

Variation of a parameter to obtain a Hopf bifurcation also makes it possible to emphasize a transition from one model to another.

Indeed, the modification of certain parameter values for a given model can be used to determine the behavior phase portrait of another model.

This comparison exhibits that the phase portrait of the Volterra-Gause model can be transformed into that of the Hastings-Powell [1991] model and vice versa.

Similarly, the phase portrait of the Rosenzweig-MacArthur [1963] model can be transformed into a “teacup” and vice versa.

The phase portrait of the Volterra-Gause model is similar to that of Rosenzweig-MacArthur [1963] in a number of respects.

These results are potentially of great value to modellers as they provide a panoply of models that are "equivalent" in terms of phase portrait but different in terms of dynamic.

\* Strictly, in the general case this model should be called the Volterra-Rosenzweig model because the functional response corresponds to that used by M.L. Rosenzweig in his famous article: *Paradox of enrichment* [Rosenzweig, 1971]. However, to avoid confusion with the Rosenzweig-MacArthur [1963] model we prefer to use the name of G.F. Gause, who was the first to use this kind of functional response but in a particular case [Gause, 1935] corresponding to the object of our study.

---

## 2. General Volterra-Gause Model

### 2.1. Model equations

We consider the Volterra-Gause model for three species interacting in a predator-prey mode.

$$\begin{aligned}\frac{dx}{dt} &= a \left(1 - \frac{\lambda}{a} x\right) x - bx^k y = xg(x) - byp(x) \\ \frac{dy}{dt} &= dx^k y - cy - ey^p z = y[-c + dp(x)] - ezy(y) \\ \frac{dz}{dt} &= (fy^p - g)z = z[-g + fq(y)]\end{aligned}\quad (1)$$

This model consists of a Verhulst [1838] logistic functional response for the prey ( $x$ ), and a Gause [1935] functional response for the predator ( $y$ ), and for the top-predator ( $z$ ).

Parameter  $a$  is the maximum per-capita growth rate for the prey in the absence of predator and  $a/\lambda$  is the carrying capacity.

The per-capita predation for the predator rate is of the Gause [1935] type.

$$p(x) = x^k$$

Parameter  $b$  is the maximum *per-capita* predation rate.

Parameter  $c$  is the per-capita natural death rate for the predator.

Parameter  $d$  is the maximum per-capita growth rate of the predator in the absence of the top-predator.

Parameters  $e$  is similar to  $b$ , except that, in each case, the predator  $y$  is the prey for the top-predator  $z$ .

### 2.2. Dynamic aspects

#### 2.2.1. Equilibrium points

The non-algebraic structure of the polynomials forming the right hand side of the equations (1) make it impossible to determine the fixed points by the classical nullclines method.

However, this model possesses two obvious fixed points: O (0, 0, 0), K ( $a/\lambda$ , 0, 0).

This makes it possible to look for fixed points within the  $xy$  plane, by fixing  $z = 0$ .

Nullcline analysis of the system (1) identifies the point I, with the following co-ordinates:

$$I \left( \left(\frac{c}{d}\right)^{\frac{1}{k}}, \frac{d}{bc} \left(\frac{c}{d}\right)^{\frac{1}{k}} \left[ a - \lambda \left(\frac{c}{d}\right)^{\frac{1}{k}} \right], 0 \right)$$

### 2.2.2. Conditions of existence of the fixed points in the xy plane (CEFP 2D)

Fixed points are only of biological importance if they are positive or null. This generates the following condition:

$$a - \lambda \left( \frac{c}{d} \right)^{\frac{1}{k}} > 0 \implies d \left( \frac{a}{\lambda} \right)^k - c > 0 \quad (2)$$

### 2.2.3. Functional Jacobian matrix

$$\mathcal{J}(\mathbf{x}, \mathbf{y}, \mathbf{z}) = \begin{pmatrix} a - b k x^{-1+k} y - 2 x \lambda & -b x^k & 0 \\ d k x^{-1+k} y & -c + d x^k - e p y^{1+p} z & -e y^p \\ 0 & f p y^{1+p} z & -g + f y^p \end{pmatrix} = \begin{pmatrix} m_{11} & m_{12} & m_{13} \\ m_{21} & m_{22} & m_{23} \\ m_{31} & m_{32} & m_{33} \end{pmatrix} \quad (3)$$

### 2.2.4. Nature and stability of the fixed points in the xy plane

The point O (0, 0, 0), with eigenvalues {a, -c, -g}, is unstable (a > 0), attractive according to y'y and z'z and repulsive according to x'x.

The point K (a / λ, 0, 0), with eigenvalues {-a, -g, -c + d (a / λ)<sup>k</sup>}, is unstable (-c + d (a / λ)<sup>k</sup> > 0, according to (2)), attractive according to x'x and z'z and repulsive according to:

$$y = - \frac{a - c + d \left( \frac{a}{\lambda} \right)^k}{b \left( \frac{a}{\lambda} \right)^k} x = -\kappa x$$

because according to (2): -c + d(a / λ)<sup>k</sup> > 0 and thus κ > 0

The method described by Freedman and Waltman [1977] can be used to study the stability of the point

$$\mathbf{I} \left( \left( \frac{c}{d} \right)^{\frac{1}{k}}, \frac{d}{bc} \left( \frac{c}{d} \right)^{\frac{1}{k}} \left[ a - \lambda \left( \frac{c}{d} \right)^{\frac{1}{k}} \right], 0 \right)$$

The characteristic polynomial of the functional Jacobian matrix can be factorised in the following form:

$$(m_{33} - \sigma) (\sigma^2 - m_{11} \sigma - m_{12} m_{21}) = 0 ; m_{13} = m_{31} = m_{32} = m_{22} = 0$$

and provides three eigenvalues: σ<sub>1</sub>, σ<sub>2</sub> and σ<sub>3</sub>

$$\sigma_1 = m_{33} = -g + f y^p \quad (4)$$

The sign of the first of these eigenvalues cannot be determined under any condition and it is therefore impossible to draw conclusions concerning the stability.

However, Hopf bifurcation in the xy plane can occur only if this eigenvalue is negative.

For the other two eigenvalues, resolution of the second-order polynomial provides a pair of eigenvalues  $\sigma_2$  and  $\sigma_3$ .

$$\sigma_{2,3} = \frac{m_{11} \pm \sqrt{\Delta}}{2} = \frac{m_{11} \pm \sqrt{m_{11}^2 + 4 m_{12} m_{21}}}{2} \quad (5)$$

If we assume that  $\Delta < 0$ , then the two eigenvalues are complex conjugated.

For Hopf bifurcation to occur, the real part of these eigenvalues must be positive and cancelled for a certain value of a parameter.

Let us choose  $\lambda$  this parameter and calculate the real part of these eigenvalues.

$$2 \operatorname{Re}[\sigma_2] = m_{11} = a - b k x^{-1+k} y - 2 x \lambda = \left[ (1 - k) \frac{bc}{d} y - \lambda x^2 \right] \left( \frac{1}{x} \right)$$

As  $a - \lambda x^2 = b x^k y$  and  $x^k = c / d$

$\operatorname{Re}[\sigma_2] > 0$  if and only if  $(1 - k)y bc/d - \lambda x^2 \geq 0$ , providing a condition for  $y$

$$y \geq \frac{d}{bc} \frac{\lambda}{1 - k} x^2$$

by replacing  $x$  and  $y$  by the co-ordinates of I

$$\lambda \leq a \left( \frac{1 - k}{2 - k} \right) \left( \frac{c}{d} \right)^{-\frac{1}{k}} \quad (6)$$

One can demonstrate that whatever the parameters of the model the discriminant  $\Delta$  is always negative. Thus the point I is always a stable or unstable focus.

### 2.2.5. Conditions for the existence of a Hopf bifurcation in the $xy$ plane

Provided that  $\lambda$  remains below this value and the first eigenvalue (4) is negative, so that the associated eigendirection is attractive and the flow is directed towards the basin of attraction of the point I, a limit cycle exists in the  $xy$  plane and a Hopf bifurcation may occur in that plane. The point

$$\mathbf{I} \left( \left( \frac{c}{d} \right)^{\frac{1}{k}}, \frac{d}{bc} \left( \frac{c}{d} \right)^{\frac{1}{k}} \left[ a - \lambda \left( \frac{c}{d} \right)^{\frac{1}{k}} \right], 0 \right)$$

is then unstable, and acts as an attractive focus in the  $xy$  plane.

### 2.2.6. Fixed points in the first octant

We will now investigate the existence of fixed points in the first octant with biological significance, i.e., for  $z > 0$ .

The non-algebraic form of the right hand side of the first equation of (1) precludes solution by means of analytical calculation.

Nevertheless, expressing this polynomial as a function of  $x$  makes it possible to specify the number of fixed points and the interval in which they belong. There are only two possible solutions to this non-algebraic polynomial.

We will call these two solutions  $x_{1,2} = \alpha$ . They lie in the following interval:

$$\mathbf{x}_1 < \mathbf{x}^* < \frac{\mathbf{a}}{\lambda} \left( \frac{1 - \mathbf{k}}{2 - \mathbf{k}} \right) < \mathbf{x}_2 < \frac{\mathbf{a}}{\lambda} \quad (7)$$

According to the third equation of (1), the second co-ordinate  $y$  can be expressed as follows:

$$(\mathbf{f} \mathbf{y}^{\mathbf{p}} - \mathbf{g}) \mathbf{z} = 0 \quad \Rightarrow \quad \mathbf{y} = \left( \frac{\mathbf{g}}{\mathbf{f}} \right)^{\frac{1}{\mathbf{p}}}$$

If we set

$$\beta = \mathbf{y} = \left( \frac{\mathbf{g}}{\mathbf{f}} \right)^{\frac{1}{\mathbf{p}}}$$

from the second equation of (1), the third co-ordinate  $z$  can be expressed in terms of  $x$ :

$$-\mathbf{c} \mathbf{y} + \mathbf{d} \mathbf{x}^{\mathbf{k}} \mathbf{y} - \mathbf{e} \mathbf{y}^{\mathbf{p}} \mathbf{z} = 0 \quad \Rightarrow \quad \mathbf{z} = \frac{\mathbf{f} \beta}{\mathbf{e} \mathbf{g}} (\mathbf{d} \mathbf{x}^{\mathbf{k}} - \mathbf{c})$$

### 2.2.7. Conditions for the existence of fixed points in the first octant (CEFP 3D)

From this third co-ordinate, another condition for the biological relevance of the fixed point can be determined.

$$\mathbf{d} \mathbf{x}^{\mathbf{k}} - \mathbf{c} > 0 \quad \Rightarrow \quad \mathbf{x} > \left( \frac{\mathbf{c}}{\mathbf{d}} \right)^{\frac{1}{\mathbf{k}}} \quad (8)$$

The fixed point  $J$  can therefore be defined in terms of all of its co-ordinates, and the conditions justifying its biological existence.

$$J \left( \alpha, \beta, \frac{\mathbf{f} \beta}{\mathbf{e} \mathbf{g}} (\mathbf{d} \alpha^{\mathbf{k}} - \mathbf{c}) \right)$$

with

$$\mathbf{x} > \left( \frac{\mathbf{c}}{\mathbf{d}} \right)^{\frac{1}{\mathbf{k}}} \quad (9)$$

A bifurcation can only occur apart from the  $xy$  plane if there is no possible bifurcation in the  $xy$  plane. This can be translated into a condition deduced from the following inequality (7):

$$\lambda \geq a \left( \frac{1-k}{2-k} \right) \left( \frac{c}{d} \right)^{-\frac{1}{k}} \Rightarrow \frac{a}{\lambda} \left( \frac{1-k}{2-k} \right) \leq \left( \frac{c}{d} \right)^{\frac{1}{k}} \quad (10)$$

By combining inequalities (7) and (9), we obtain:

$$\mathbf{x}_1 < \mathbf{x}^* < \frac{a}{\lambda} \left( \frac{1-k}{2-k} \right) < \left( \frac{c}{d} \right)^{\frac{1}{k}} < \mathbf{x}_2 < \frac{a}{\lambda} \quad (11)$$

### 2.2.8. Nature and stability of the fixed points in the first octant

The method described by Freedman and Waltman [1977] can still be used to investigate the stability of the point

$$\mathcal{J} \left( \alpha, \beta, \frac{\mathbf{f}\beta}{\mathbf{e}\mathbf{g}} (d\alpha^k - c) \right)$$

According to this method, if  $m_{11} > 0$ , then the point J is unstable.

If  $m_{11} < 0$  and  $m_{22} \leq 0$ , then the point J is stable.

Furthermore, if  $m_{11} < 0$ , then the point J is asymptotically stable.

The trace and the determinant of the functional Jacobian matrix evaluated at point J give:

$$\begin{aligned} \sigma_1 + \sigma_2 + \sigma_3 &= \mathbf{Tr}[\mathcal{J}] = m_{11} + m_{22} \\ &= a(1-k) - \lambda \mathbf{x}(2-k) + (1-p)(-c + d\mathbf{x}^k) \\ \sigma_1 \sigma_2 \sigma_3 &= \mathbf{Det}[\mathcal{J}] = m_{11} m_{23} m_{32} \\ &= [a(1-k) - \lambda \mathbf{x}(2-k)] [\mathbf{e}\mathbf{g}\mathbf{p}\mathbf{y}^{p-1} \mathbf{z}] \\ &= [a(1-k) - \lambda \mathbf{x}(2-k)] (-c + d\mathbf{x}^k) \mathbf{g}\mathbf{p} \end{aligned}$$

### 2.2.9. Conditions for the existence of a Hopf bifurcation in the first octant

Based on the conditions for the biological existence of a fixed point J (CEFP 3D), we can conclude:

If  $x_1$  is the solution of the first nullcline, then the point J does not exist because, according to condition (11),  $x_1 < (c/d)^{1/k}$  and therefore  $z_1 < 0$ . A Hopf bifurcation may then occur at point I in the  $xy$  plane if the first eigenvalue (4) is negative. In this case, the associated eigendirection is attractive and the flow is directed towards the basin of attraction of the point I. This is consistent with condition (6), which implies that:

$$\mathbf{x}_1 < \left( \frac{c}{d} \right)^{\frac{1}{k}} < \mathbf{x}^* < \frac{a}{\lambda} \left( \frac{1-k}{2-k} \right)$$

If  $x_2$  is the solution of the first nullcline, then the point J exists because according to the condition (11),

$$\mathbf{x}_1 < \mathbf{x}^* < \frac{\mathbf{a}}{\lambda} \left( \frac{1 - \mathbf{k}}{2 - \mathbf{k}} \right) < \left( \frac{\mathbf{c}}{\mathbf{d}} \right)^{\frac{1}{\mathbf{k}}} < \mathbf{x}_2 < \frac{\mathbf{a}}{\lambda}$$

In this case, points I and J co-exist and it is necessary to determine the stability of J, even if the first eigenvalue (4) is positive, resulting in the associated eigendirection being repulsive and the flow being directed towards the basin of attraction of the point J.

Nevertheless in this precise case:  $m_{11} = a(1 - k) - \lambda x_2(2 - k) < 0$ .

This implies that the determinant is negative and the sign of the trace is unspecified because we deal with a difference.

If we assume that the characteristic polynomial of the functional Jacobian matrix has two complex conjugated eigenvalues, the trace and the determinant will be written:

$$\begin{aligned} \sigma_1 + 2 \operatorname{Re}[\sigma_2] &= \operatorname{Tr}[\mathcal{J}] \\ \sigma_1 | \sigma_2 |^2 &= \operatorname{Det}[\mathcal{J}] < 0 \end{aligned}$$

We can deduce from these expressions that the first eigenvalue is negative. Thus the associated eigendirection is attractive and the flow is directed towards the basin of attraction of the point J. Moreover, the indeterminate nature of the sign of the trace is consistent with the possibility that the real part of the eigenvalues can change. Thus, in this case, the possibility of Hopf bifurcation apart from the  $xy$  plane may be considered.

## 2.3. Volterra-Gause model for $k = p = 1/2$

### 2.3.1. Dimensionless equations

Expressing equations in a dimensionless form makes it possible to reduce the number of parameters of the model.

Let us assume:

$$\begin{aligned} \mathbf{x} &\rightarrow \frac{\mathbf{a}}{\lambda} \mathbf{x} \\ \mathbf{y} &\rightarrow \frac{\mathbf{a}}{\mathbf{b}} \left( \frac{\mathbf{a}}{\lambda} \right)^{\frac{1}{2}} \mathbf{y} \\ \mathbf{z} &\rightarrow \frac{\mathbf{d}}{\mathbf{e}} \left( \frac{\mathbf{a}}{\mathbf{b}} \right)^{\frac{1}{2}} \left( \frac{\mathbf{a}}{\lambda} \right)^{\frac{3}{4}} \mathbf{z} \\ \mathbf{t} &\rightarrow \frac{\mathbf{t}}{\mathbf{d} \left( \frac{\mathbf{a}}{\lambda} \right)^{\frac{1}{2}}} \end{aligned}$$

and

$$\delta_1 = \frac{c}{d} \frac{1}{\left(\frac{a}{\lambda}\right)^{\frac{1}{2}}}$$

$$\delta_2 = \frac{1}{f} \frac{g}{\left[\frac{a}{b} \left(\frac{a}{\lambda}\right)^{\frac{1}{2}}\right]^{\frac{1}{2}}}$$

$$\xi = \frac{d}{a} \left(\frac{a}{\lambda}\right)^{\frac{1}{2}}$$

$$\varepsilon = \frac{f}{d} \frac{\left(\frac{a}{b}\right)^{\frac{1}{2}}}{\left(\frac{a}{\lambda}\right)^{\frac{1}{4}}}$$

This generates a dimensionless model with four parameters instead of eight. In fact, as we have decided to set  $k = p = 1/2$ , the final model actually has six parameters rather than eight.

$$\begin{aligned} \xi \frac{dx}{dt} &= x(1-x) - x^{\frac{1}{2}}y \\ \frac{dy}{dt} &= -\delta_1 y + x^{\frac{1}{2}}y - y^{\frac{1}{2}}z \quad (12) \\ \frac{dz}{dt} &= \varepsilon \left( y^{\frac{1}{2}} - \delta_2 \right) z \end{aligned}$$

### 2.3.2. Fixed points of dimension in the $xy$ plane

The two previously identified fixed points are again found: O (0, 0, 0) and K (1, 0, 0). In addition, the setting of the  $k$  and  $p$  parameters makes it possible to solve the first nullcline simply by changing variable. However, the method developed above remains valid and exact knowledge of the solutions of this equation is not necessary for determination of the stability of the fixed points. It is therefore possible to look for fixed points in the  $xy$  plane by setting  $z = 0$  for  $k = p = 1/2$ . This gives the following co-ordinates of point I:

$$\mathbf{I} (\delta_1^2, \delta_1 (1 - \delta_1^2), 0)$$

### 2.3.3. Conditions for the existence of fixed points in the $xy$ plane (CEFP 2D)

Fixed points are only of biological significance if they are positive or null. This generates the following condition:

$$1 - \delta_1^2 > 0 \quad \Rightarrow \quad \delta_1 < 1 \quad (13)$$

### 2.3.4. Functional Jacobian matrix

$$\mathcal{J}(x, y, z) = \begin{pmatrix} \frac{1}{\xi} \left( 1 - 2x - \frac{1}{2} \frac{y}{\sqrt{x}} \right) & -\frac{1}{\xi} \sqrt{x} & 0 \\ \frac{1}{2} \frac{y}{\sqrt{x}} & \sqrt{x} - \frac{1}{2} \frac{z}{\sqrt{y}} - \delta_1 & -\sqrt{y} \\ 0 & \frac{1}{2} \varepsilon \frac{z}{\sqrt{y}} & \varepsilon (\sqrt{y} - \delta_2) \end{pmatrix} = \begin{pmatrix} m_{11} & m_{12} & m_{13} \\ m_{21} & m_{22} & m_{23} \\ m_{31} & m_{32} & m_{33} \end{pmatrix} \quad (14)$$

### 2.3.5. Nature and stability of the fixed points in the xy plane

The point O (0, 0, 0), with the eigenvalues  $\{1/\xi, -\delta_1, -\varepsilon\delta_2\}$ , is unstable ( $1/\xi > 0$ ), and the eigendirections associated with the eigenvalues  $-\delta_1, -\varepsilon\delta_2$  are attractive according to  $y'y$  and  $z'z$  and repulsive according to  $x'x$  for  $1/\xi$ .

The point K (1, 0, 0), with the eigenvalues  $\{-1/\xi, 1-\delta_1, -\varepsilon\delta_2\}$ , is unstable ( $1-\delta_1 > 0$ , according to (10)), and the eigendirections associated with the eigenvalues  $-1/\xi, -\varepsilon\delta_2$  are attractive according to  $x'x$  and  $z'z$  and repulsive according to the direction of the straight line defined by the following equation:

$$y = -[\xi(1 - \delta_1) + 1] x$$

The method of Freedman and Waltman[1977] can again be used to assess the stability of the point

$$\mathbf{I}(\delta_1^2, \delta_1(1 - \delta_1^2), 0)$$

The characteristic polynomial of the functional Jacobian matrix can be factorised in the following form:

$$(m_{33} - \sigma) (\sigma^2 - m_{11}\sigma - m_{12}m_{21}) = 0 ; m_{13} = m_{31} = m_{32} = m_{22} = 0$$

and provides three eigenvalues:  $\sigma_1, \sigma_2$  and  $\sigma_3$

$$\sigma_1 = m_{33} = \varepsilon \left[ \delta_1^2 \left( 1 - \delta_1^2 \right)^{\frac{1}{2}} - \delta_2 \right] \quad (15)$$

For the first eigenvalue, the conditions for the existence of a fixed point in the first octant (CEFP 3D) make it possible to define the sign of the eigenvalue, and therefore to draw conclusions concerning the stability. For the other two eigenvalues, resolution of the second-order polynomial gives a pair of eigenvalues,  $\sigma_2$  and  $\sigma_3$ .

$$\sigma_{2,3} = \frac{m_{11} \pm \sqrt{\Delta}}{2} = \frac{m_{11} \pm \sqrt{m_{11}^2 + 4m_{12}m_{21}}}{2} \quad (16)$$

If we assume that  $\Delta < 0$ , then the two eigenvalues are then complex conjugated.

For Hopf bifurcation to occur, the real part of these eigenvalues must be positive and cancelled for a certain value of a parameter.

Let us choose  $\delta_1$  this parameter and calculate the real part of these eigenvalues.

$$2 \operatorname{Re}[\sigma_2] = m_{11} = \frac{1}{\xi} (1 - 3\delta_1^2) \geq 0 \implies \delta_1 \leq \frac{1}{\sqrt{3}} \quad (17)$$

For this bifurcation occurs in the  $xy$  plane, the first eigenvalue (15) must be negative, so that the associated eigendirection is attractive and the flow is directed towards the basin of attraction of point I.

If this eigenvalue is considered as a function of  $\delta_1$ , one can show that it will remain negative provided that:

$$\delta_2 \geq \sqrt{\frac{2}{3\sqrt{3}}} \quad (18)$$

This condition rules out the existence of a point J in the first octant.

### 2.3.6. Conditions for the existence of a Hopf bifurcation in the $xy$ plane

If conditions (17) and (18) are met, a limit cycle exists in the  $xy$  plane and a Hopf bifurcation may occur in that plane. Point J of dimension three cannot exist and the point  $I(\delta_1^2, \delta_1(1-\delta_1^2), 0)$  is unstable. It acts as an attractive focus in the  $xy$  plane.

### 2.3.7. Fixed points in the first octant

We will now focus on the existence of fixed points of biological importance in the first octant, i.e., for  $z > 0$ . We can specify the number of solutions of the non-algebraic polynomial of the first equation (12) and the interval in which they lie as described above.

We will once again call the two possible solutions  $x_{1,2} = \alpha$  these solutions. These solutions lie in the following interval:

$$0 < \mathbf{x}_1 < \mathbf{x}^* < \frac{1}{3} < \mathbf{x}_2 < 1$$

Mathematical study of the first nullcline as a function of  $x$  generates the following condition for the existence of the fixed points in the first octant (CEFP 3D):

$$\delta_2 \leq \sqrt{\frac{2}{3\sqrt{3}}} \quad (19)$$

From the third equation of (12), the second co-ordinate  $y$  may be expressed as follows:

$$\varepsilon \left( \mathbf{y}^{\frac{1}{2}} - \delta_2 \right) = 0 \implies \mathbf{y} = \delta_2^2$$

From the second equation of (12), the third co-ordinate  $z$  can be expressed in terms of  $x$ :

$$-\delta_1 \mathbf{y} + \mathbf{x}^{\frac{1}{2}} \mathbf{y} - \mathbf{y}^{\frac{1}{2}} \mathbf{z} = 0 \implies \mathbf{z} = \delta_2 \left( \mathbf{x}^{\frac{1}{2}} - \delta_1 \right)$$

### 2.3.8. Conditions for the existence of fixed points in the first octant (CEFP 3D)

From this third co-ordinate, we can deduce another condition for the biological existence of the fixed point:

$$\mathbf{x}^{\frac{1}{2}} - \delta_1 > 0 \implies \mathbf{x} > \delta_1^2 \quad (20)$$

The fixed point J can therefore be defined in terms of its co-ordinates in all three dimensions and the conditions justifying its biological existence.

$$\mathcal{J} \left( \alpha, \delta_2^2, \delta_2 \left( \alpha^{\frac{1}{2}} - \delta_1 \right) \right)$$

with

$$\mathbf{x} > \delta_1^2 \quad (21)$$

If a bifurcation is to occur apart from the  $xy$  plane, bifurcation must not be possible in the  $xy$  plane. This translates into a condition that can be deduced from inequality (17):

$$\delta_1 > \frac{1}{\sqrt{3}}$$

or

$$\frac{1}{\sqrt{3}} > \frac{1}{3}$$

By combining inequalities (20) and (21), we obtain:

$$\mathbf{x}_1 < \mathbf{x}^* < \frac{1}{3} < \delta_1 < \mathbf{x}_2 < 1 \quad (22)$$

### 2.3.9. Nature and stability of the fixed points in the first octant

The method of Freedman and Waltman [1977] can be used to study the stability of the point

$$\mathcal{J} \left( \alpha, \delta_2^2, \delta_2 \left( \alpha^{\frac{1}{2}} - \delta_1 \right) \right)$$

According to this method, if  $m_{11} > 0$ , then the point J is unstable.

If  $m_{11} < 0$  and  $m_{22} \leq 0$ , then the point J is stable.

Furthermore, if  $m_{11} < 0$ , then the point J is asymptotically stable.

The trace and the determinant of the functional Jacobian matrix evaluated at point J give:

$$\begin{aligned}\sigma_1 + \sigma_2 + \sigma_3 &= \mathbf{Tr}[\mathcal{J}] = m_{11} + m_{22} = \frac{1}{2\xi} (1 - 3\mathbf{x}) + \frac{1}{2} \left( \mathbf{x}^2 - \delta_1 \right) \\ \sigma_1 \sigma_2 \sigma_3 &= \mathbf{Det}[\mathcal{J}] = m_{11} m_{23} m_{32} = \frac{\varepsilon}{2\xi} (1 - 3\mathbf{x}) \mathbf{z}\end{aligned}$$

### 2.3.10. Conditions for the existence of a Hopf bifurcation in the first octant

From the conditions for the biological existence of the fixed point J (CEFP 3D), we can conclude:

If  $x_1$  is the solution of the first nullcline, then point J does not exist because according to condition (22),  $x_1 < \delta_1$  and therefore  $z_1 < 0$ .

A Hopf bifurcation may occur in the  $xy$  plane at point I if the first eigenvalue (15) is negative. In this case, the associated eigendirection is attractive and the flow is directed towards the basin of attraction of point I, consistent with condition (17), which implies that:

$$\mathbf{x}_1 < \delta_1 < \mathbf{x}^* < \frac{1}{3}$$

If  $x_2$  is the solution of the first nullcline, then the point J exists because according to condition (22),

$$0 < \mathbf{x}_1 < \mathbf{x}^* < \frac{1}{3} < \delta_1 < \mathbf{x}_2 < 1$$

In this case, points I and J co-exist and it is necessary to determine the stability of J, even if the first eigenvalue (15) is positive, resulting in the associated eigendirection being repulsive and the flow being directed towards the basin of attraction of the point J.

Nevertheless in this precise case:  $1 - 3x < 0$ .

This implies that the determinant is negative and the sign of the trace is unspecified as we are dealing with a difference.

If we assume that the characteristic polynomial of the functional Jacobian matrix has two conjugated complex eigenvalues, then the trace and the determinant can be expressed as follows:

$$\begin{aligned}\sigma_1 + 2 \operatorname{Re}[\sigma_2] &= \mathbf{Tr}[\mathcal{J}] \\ \sigma_1 | \sigma_2 |^2 &= \mathbf{Det}[\mathcal{J}] < 0\end{aligned}$$

We can deduce from this that the first eigenvalue is negative, so the associated eigendirection is attractive and the flow is directed towards the basin of attraction of the point J. Moreover, the indeterminate nature of the sign of the trace makes it possible for the real part of the eigenvalues to change. Hopf bifurcation apart from the  $xy$  plane may therefore be considered.

### 2.3.11. Bifurcation parameter value

Numerically, the value of the selected bifurcation parameter can be calculated with a high level of accuracy. The technique used involves calculating the fixed points according to the parameter and evaluating the eigenvalues of the functional Jacobian matrix at this point. These eigenvalues are thus themselves a function of the selected parameter. Their real parts can therefore be expressed as a function of this parameter, making it possible to determine the value for which two of these eigenvalues cancel out, corresponding to the value of the bifurcation parameter. Applied to system (12) by setting  $\xi = 0.866$ ,  $\varepsilon = 1.428$ ,  $\delta_2 = 0.376$ , we obtained for the parameter  $\delta_1$ :

$$\delta_1 = 0.747413$$

### 2.3.12. Phase portrait

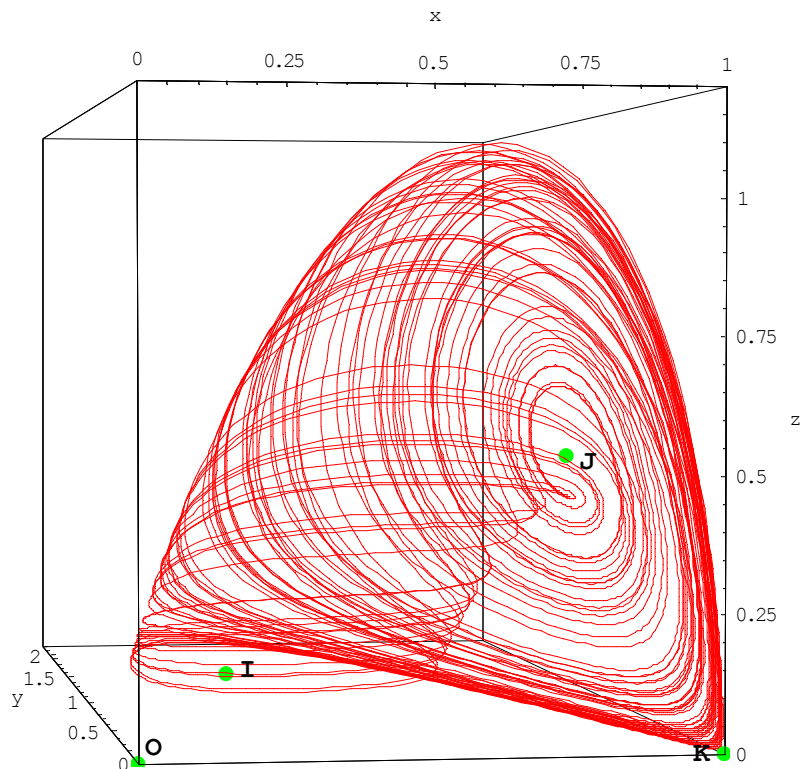


Fig. 1. Phase portrait of system (12). The chaotic attractor takes the shape of a snail shell. Parameter values are:  $\xi = 0.866$ ,  $\varepsilon = 1.428$ ,  $\delta_1 = 0.577$ ,  $\delta_2 = 0.376$ .

Despite its familiar appearance, this attractor behaves in a complex manner. Starting from any initial condition in the first octant, the flow is directed towards point K, which is attractive according to the  $x$  eigendirection.

Following the repulsive eigendirection  $y = -[\xi(1 - \delta_1) + 1]x$  of the point K, the flow reaches the basin of attraction of the point I, which exhibits an attractive focus behaviour in the  $xy$  plane and turns around the point I.

However, as this point has a repulsive eigendirection, the flow leaves the  $xy$  plane and moves towards the basin of attraction of the point J which has an attractive eigendirection.

As the point J behaves as a repulsive focus, the flow turns around this point while moving away in the direction of the point K which has an attractive eigendirection according to  $z/z$ .

The flow is therefore "reinjected" by this "saddle-point".

### 2.3.13. Bifurcation diagrams

As pointed out by Glass and Mackey [1988], the construction of a bifurcation diagram is a good means of locating the signature of chaos in a system.

We present below the bifurcation diagram of the dimensionless system (12) to highlight the period doubling induced by the parameter  $\delta_1$ .

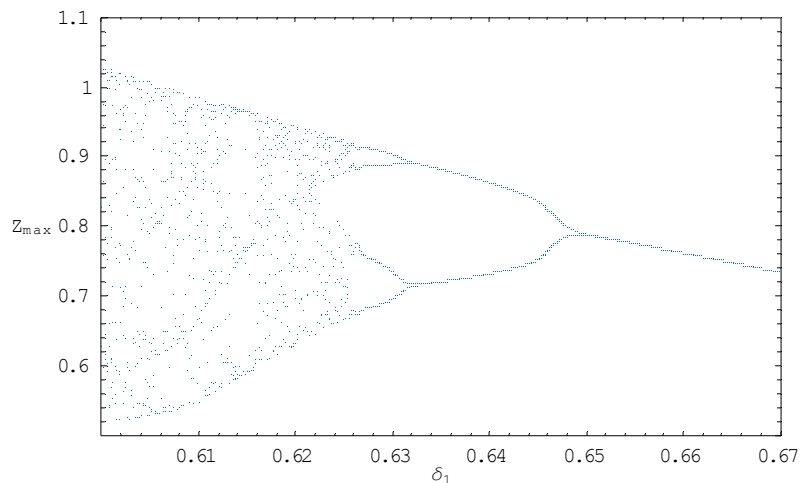


Fig. 2. Bifurcation diagram of system (12) for the parameter  $\delta_1$ ;  $z_{\max} = f(\delta_1)$

### 2.3.13. Poincaré section and Poincaré map

The Poincaré section corresponds here to a plane with  $z = 1/2$ , i.e., a plane dividing the snail shell into two parts. It therefore consists of a set of  $x$  and  $y$  values.

Taking  $x(n)$  as the value of  $x$  at the  $n$ th intersection of the trajectory with the Poincaré section, we can construct the Poincaré map: the function relating  $x(n+1)$  to  $x(n)$

In Fig. 3., we can see that the slope of the multimodal Poincaré map is steep, a feature typical of chaos.

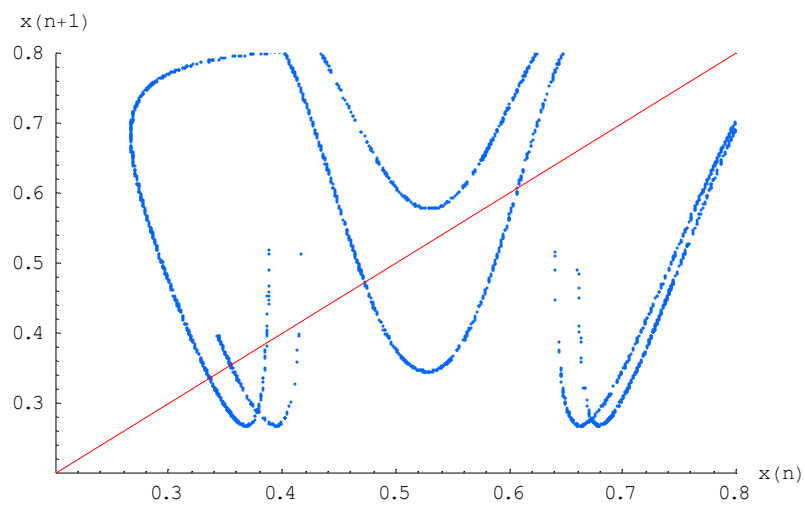


Fig. 3. Poincaré map of system (12) for the same parameters

## 2.4. Slow-fast dynamics

Given all the conditions for the existence of fixed points (CEFP 2D & 3D), it is reasonable to assume "trophic time diversification" occurs, implying that:

$$\mathbf{a} > \mathbf{d} > \mathbf{f}$$

i.e., *the maximum per-capita growth rate decreases from the bottom to the top of the food chain.*

We can then consider the case in which:

$$\mathbf{a} \gg \mathbf{d} \gg \mathbf{f}$$

or

$$0 < \xi \ll 1$$

and

$$0 < \varepsilon \ll 1$$

Under these conditions, system (12) becomes a singularly perturbed system of three time scales. The rates of change for the prey, the predator and top-predator from fast to intermediate to slow, respectively [B.Deng,2001]. Based on the works of Ramdani *et al.*, [2000], we consider system (12) to be a slow-fast autonomous dynamic system defined by a slow manifold equation on which the attractor lies. A state equation binding the three variables can then be established.

### 2.4.1. Slow manifold equation based on the orthogonality principle

Using the method developed by Ramdani *et al.*, [2000], we can obtain the slow manifold equation defined by the layer of planes locally orthogonal to the fast eigenvector on the left.

$$\lambda_1(\mathbf{x}, \mathbf{y}, \mathbf{z}) \mathbf{z}_{\lambda_1}(1, \beta(\mathbf{x}, \mathbf{y}, \mathbf{z}), \gamma(\mathbf{x}, \mathbf{y}, \mathbf{z}))$$

Let us call  $\lambda_1(\mathbf{x}, \mathbf{y}, \mathbf{z})$  the fast eigenvalue of  $\mathcal{J}(\mathbf{x}, \mathbf{y}, \mathbf{z})$  and  $\mathbf{z}_{\lambda_1}(1, \beta(\mathbf{x}, \mathbf{y}, \mathbf{z}), \gamma(\mathbf{x}, \mathbf{y}, \mathbf{z}))$  the fast eigenvectors on the left of  $\mathcal{J}(\mathbf{x}, \mathbf{y}, \mathbf{z})$ .

Transposing the characteristic equation,

$${}^t(\mathcal{J}(\mathbf{x}, \mathbf{y}, \mathbf{z})) \mathbf{z}_{\lambda_1}(\mathbf{x}, \mathbf{y}, \mathbf{z}) = \lambda_1(\mathbf{x}, \mathbf{y}, \mathbf{z}) \mathbf{z}_{\lambda_1}(\mathbf{x}, \mathbf{y}, \mathbf{z})$$

we can find  $\beta$  and  $\gamma$ .

$$\beta = \frac{1}{\frac{1}{2} \mathbf{x}^{-\frac{1}{2}} \mathbf{y}} \left( \lambda_1 - \frac{1}{\xi} \left( 1 - 2\mathbf{x} - \frac{1}{2} \mathbf{x}^{-\frac{1}{2}} \mathbf{y} \right) \right)$$

$$\gamma = \beta \frac{\mathbf{y}^{\frac{1}{2}}}{\varepsilon \left( \mathbf{y}^{\frac{1}{2}} - \delta_2 \right) - \lambda_1}$$

The slow manifold equation is thus given by:

$$\dot{\mathbf{x}} + \beta(\mathbf{x}, \mathbf{y}, \mathbf{z}) \dot{\mathbf{y}} + \gamma(\mathbf{x}, \mathbf{y}, \mathbf{z}) \dot{\mathbf{z}} = \mathbf{0} \quad (23)$$

This leads to an implicit equation which can be simulated numerically. We have used *Mathematica* software in this study.

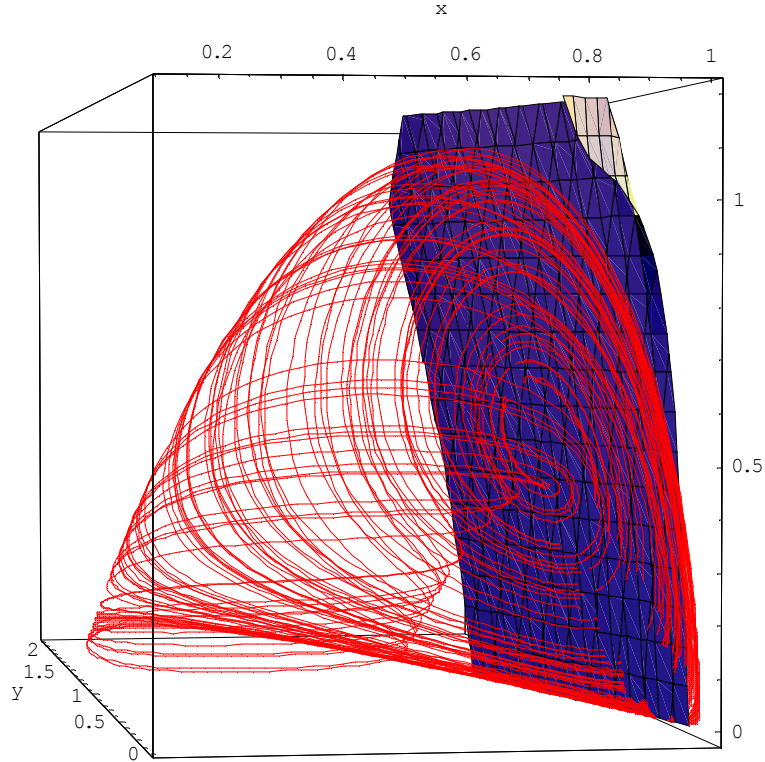


Fig. 4. Slow manifold surface based on the orthogonality principle and phase portrait of the Volterra-Gause system (12) with the same parameter values. In this figure, we can see the slow manifold on which the solutions of the system (12) are based.

#### 2.4.2. Slow manifold equation based on the slow eigenvectors

The slow manifold equation could also have been obtained as described by Ramdani *et al.*, [2000], by assuming that the three components of the system (12) are always parallel to a plane containing the two slow eigenvectors.

## **2.5. Conclusion**

This work demonstrates the presence of chaos in a Volterra-Gause model of predator-prey type. Nevertheless, a more profound mathematical approach, such as investigation of the possible existence of Shilnikov orbits, should make it possible to confirm the presence of chaos in this system. Our work has also demonstrated that this model has five key characteristics:

- Presence of limit cycles
- Existence of Hopf bifurcation
- Chaos by period doubling cascade
- Slow-fast dynamics
- Existence of a slow manifold on which the attractor lies.

The Volterra-Gause model is also similar to other models, such as those of Rosenzweig-MacArthur and Hastings and Powell. These similarities will be considered in the next section.

## 3. Similarity to the Rosenzweig-MacArthur and Hastings-Powell Models

### 3.1. Rosenzweig-MacArthur model

We considered the Rosenzweig-MacArthur model [1963] for a three trophic level interaction involving a prey ( $x$ ), a predator ( $y$ ) and a top-predator ( $z$ ).

$$\begin{aligned}\frac{dx}{dt} &= a \left(1 - \frac{\lambda}{a} x\right) x - \frac{bxy}{H_1 + x} = xg(x) - byp(x) \\ \frac{dy}{dt} &= y \left( \frac{dx}{H_1 + x} - c \right) - \frac{eyz}{H_2 + y} = y[-c + dp(x)] - ezy(y) \quad (24) \\ \frac{dz}{dt} &= z \left( \frac{fy}{H_2 + y} - g \right) = z[-g + fq(y)]\end{aligned}$$

This model includes a Verhulst [1838] logistic prey ( $x$ ), a Holling [1959] *type 2* predator ( $y$ ), and a Holling [1959] *type 2* top-predator ( $z$ ).

Parameter  $a$  is the maximum per-capita growth rate for the prey in the absence of predator and  $K = a / \lambda$  is the carrying capacity.

The per-capita predation rate of the predator has the Holling [1959] *type 2* form.

$$p(x) = \frac{bx}{H_1 + x}$$

Parameter  $b$  is the maximum *per-capita* predation rate and  $H_1$  is the semi-saturation constant at which the per-capita predation rate is half its maximum,  $b/2$ .

Parameter  $c$  is the per-capita natural death rate for the predator.

Parameter  $d$  is the maximum per-capita growth rate of the predator in the absence of the top-predator.

Parameters  $e$  and  $H_2$  are similar to  $b$  and  $H_1$ , except that the predator  $y$  is the prey for the top-predator  $z$ . Parameters  $f$  and  $g$  are similar to  $c$  and  $d$ , except that the predator  $y$  is the prey for the top-predator  $z$ .

Note that the Rosenzweig-MacArthur model was developed from the seminal works of Lotka [1925] and Volterra [1926].

#### 3.1.1. Dimensionless equations

With the following changes of variables and parameters,

$$\begin{aligned}t &\rightarrow dt, \quad x \rightarrow \frac{\lambda}{a} x, \quad y \rightarrow \frac{b\lambda}{a^2} y, \quad z \rightarrow \frac{be\lambda}{da^2} z, \\ \xi &= \frac{d}{a}, \quad \varepsilon = \frac{f}{d}, \quad \beta_1 = \frac{\lambda H_1}{a}, \quad \beta_2 = \frac{H_2}{Y_0}, \\ Y_0 &= \frac{a^2}{b\lambda}, \quad \delta_1 = \frac{c}{d}, \quad \delta_2 = \frac{g}{f}\end{aligned}$$

### 3.1.2. Biological hypothesis

We have made several assumptions to provide biological reality to our study:

- Positivity of the fixed points
- "Trophic time diversification hypothesis" such that the maximum per-capita growth rate decreases from the bottom to the top of the food chain as follows

$$\mathbf{a} > \mathbf{d} > \mathbf{f} > \mathbf{0}$$

We also assumed major changes over time

$$\mathbf{a} \gg \mathbf{d} \gg \mathbf{f} > \mathbf{0} \quad (25)$$

Detailed comments on changes in variables and parameters were made in the paper by Deng [2001]. For technical reasons, both  $y$  and  $z$  were rescaled by a factor of 0.25:

$$y \rightarrow y / 0.25 ; z \rightarrow z / 0.25$$

Equations (24) have been reformulated in the following dimensionless form:

$$\begin{aligned} \varepsilon \frac{d\mathbf{x}}{d\mathbf{t}} &= \mathbf{x} \left( \mathbf{1} - \mathbf{x} - \frac{\mathbf{y}}{\beta_1 + \mathbf{x}} \right) \\ \frac{d\mathbf{y}}{d\mathbf{t}} &= \mathbf{y} \left( \frac{\mathbf{x}}{\beta_1 + \mathbf{x}} - \delta_1 - \frac{\mathbf{z}}{\beta_2 + \mathbf{y}} \right) \\ \frac{d\mathbf{z}}{d\mathbf{t}} &= \varepsilon \mathbf{z} \left( \frac{\mathbf{y}}{\beta_2 + \mathbf{y}} - \delta_2 \right) \end{aligned} \quad (26)$$

### 3.1.3. Dynamic aspects

Under these conditions (25), the system (26) becomes a singularly perturbed system of three time scales, as previously pointed out by several authors [Kuznetsov, 1995, Muratori & Rinaldi, 1992, Rinaldi & Muratori, 1992]. The rates of change for the prey, the predator and the top-predator range from fast to intermediate to slow, respectively [B. Deng, 2001]. Based on the works of Ramdani *et al.*, [2000], we consider the system (26) to be a slow-fast autonomous dynamic system and provide the equation for the slow manifold on which the attractor lies. A state equation binding the three variables can also be established.

#### *Nature and stability of the fixed points*

For the set of values initially used in this simulation ( $\varepsilon = 0.1, \beta_1 = 0.3, \beta_2 = 0.1, \delta_1 = 0.1, \delta_2 = 0.62, \varepsilon = 0.3$ ), we obtain four equilibrium points (of biological significance) with the following eigenvalues:

$$\text{O} (0, 0, 0) \rightarrow \{10, -0.186, -0.1\}$$

$$\text{I} (0.033, 1.289, 0) \rightarrow \{0.314194 + 0.878508 i, 0.314194 - 0.878508 i, 0.0429782\}$$

$$\text{J} (0.859, 0.652, 0.674) \rightarrow \{-7.51526, 0.18173 + 0.111807 i, 0.18173 - 0.111807 i\}$$

$$\text{K} (1, 0, 0) \rightarrow \{-10, 0.669231, -0.186\}$$

So according to the Lyapunov criterion, all these points are unstable.

The literal expression of the fixed points highlights their dependence on the parameters considered.

We use this result below to calculate the Hopf bifurcation parameter.

*Phase portrait and vectorfield portrait*

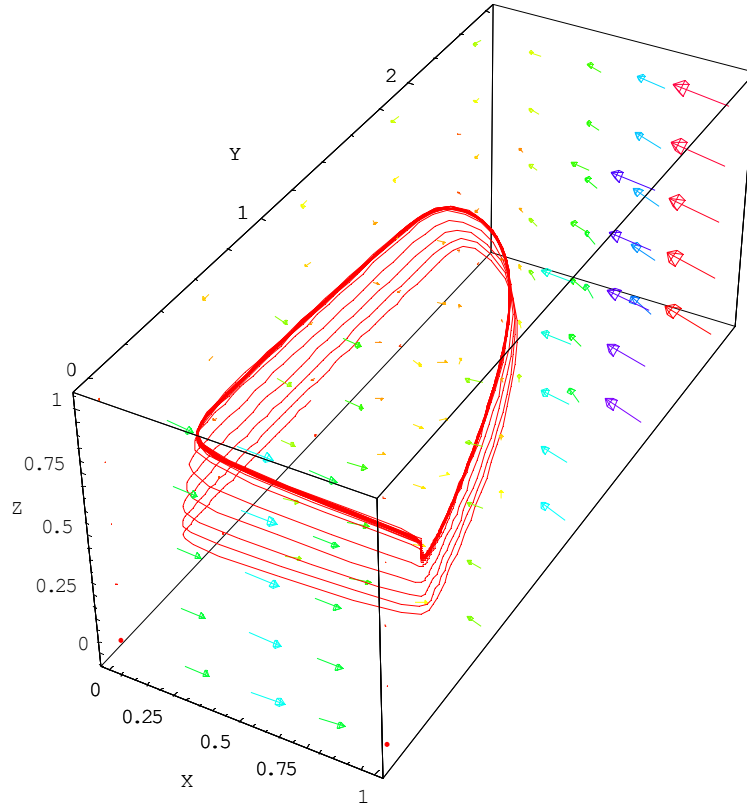


Fig. 5. Phase and vectorfield portrait of the Rosenzweig-MacArthur system (26) with the same parameter values.

This figure shows slow-fast dynamic features, with long arrow for the fast features and short arrows for the slow features. This portrait consists of four branches: two fast (the shorter branches) and two slow (the longer branches). The pattern of change in this attractor resembles that of the original Volterra model. In initial, fast part of the attractor, the prey ( $x$ ) rapidly increase in number, whereas the number of predators ( $y$ ) and top-predators ( $z$ ) remain very low. This situation realistic. Close to the equilibrium point I, the number of top-predators suddenly decreases, triggering an increase in the predator population. In the second part of the attractor, a slow stage, the number of predators increases, as does the number of top-predators, whereas the number of prey decreases. This part of the attractor leads on to another slow stage, during which the number of predators is maximal. This results in a decrease in the number of prey. In the fourth part of the attractor, a slow stage, the number of top-predators continues to increase while the number of predators decreases. As demonstrated by Deng [Deng, 2001], this attractor with a Moebius strip shape displays chaotic behaviour.

### 3.1.4. Slow manifold equation

*Slow manifold equation based on the orthogonality principle*

As described in Sec. 2.4., the slow manifold equation can be expressed as follows:

$$\lambda_1(\mathbf{x}, \mathbf{y}, \mathbf{z}) \mathbf{z}_{\lambda_1}(\mathbf{1}, \beta(\mathbf{x}, \mathbf{y}, \mathbf{z}), \gamma(\mathbf{x}, \mathbf{y}, \mathbf{z}))$$

Let us call  $\lambda_1(x, y, z)$  the fast eigenvalue of  $\mathcal{J}(x, y, z)$  and  $\mathbf{z}_{\lambda_1}(1, \beta(x, y, z), \gamma(x, y, z))$  the fast eigenvectors to the left of  $\mathcal{J}(x, y, z)$ .

Transposing the characteristic equation,

$${}^t(\mathcal{J}(\mathbf{x}, \mathbf{y}, \mathbf{z})) \mathbf{z}_{\lambda_1}(\mathbf{x}, \mathbf{y}, \mathbf{z}) = \lambda_1(\mathbf{x}, \mathbf{y}, \mathbf{z}) \mathbf{z}_{\lambda_1}(\mathbf{x}, \mathbf{y}, \mathbf{z})$$

we can find  $\beta$  and  $\gamma$ .

$$\beta = \frac{(\mathbf{x} + \beta_1)^2}{\beta_1 \mathbf{y}} \left[ \lambda_1 - \frac{1}{\xi} \left( 1 - 2\mathbf{x} - \frac{0.25 \mathbf{y} \beta_1}{(\mathbf{x} + \beta_1)^2} \right) \right]$$

$$\gamma = \beta \frac{\frac{0.25 \mathbf{y}}{0.25 \mathbf{y} + \beta_2}}{\varepsilon \left( \frac{0.25 \mathbf{y}}{0.25 \mathbf{y} + \beta_2} - \delta_2 \right) - \lambda_1}$$

$$\dot{\mathbf{x}} + \beta(\mathbf{x}, \mathbf{y}, \mathbf{z}) \dot{\mathbf{y}} + \gamma(\mathbf{x}, \mathbf{y}, \mathbf{z}) \dot{\mathbf{z}} = 0 \quad (27)$$

This leads to an implicit equation which can be simulated numerically.

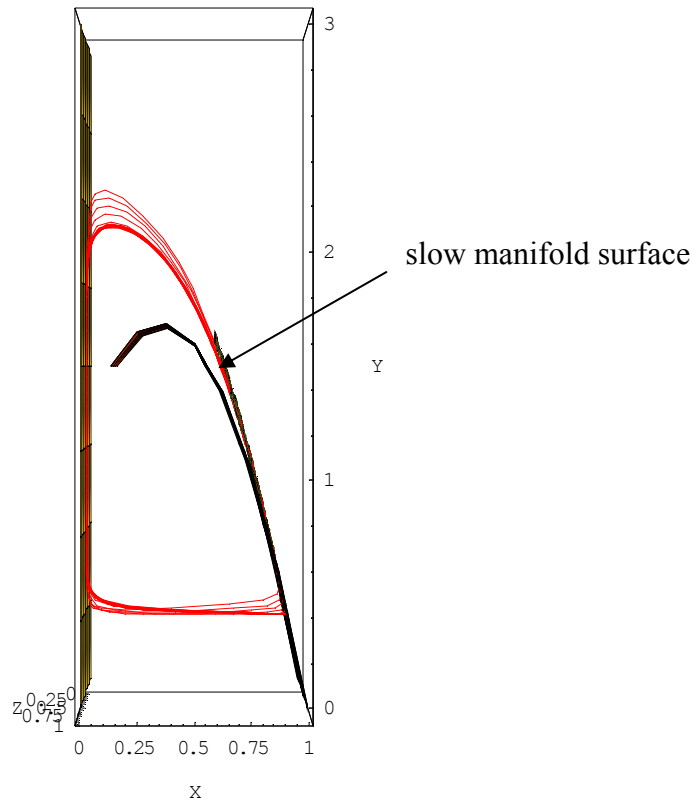


Fig. 6. Slow manifold surface defined according to the orthogonality principle. Nullcline surface corresponding to the singular perturbation and phase portrait of the Rosenzweig-MacArthur system (26), with the same parameter values. We seen here the slow manifold on which the solutions of the system (26) are based.

#### *Slow manifold equation based on the slow eigenvectors*

The slow manifold equation can be also obtained by means of the slow eigenvectors method.

#### *3.1.5. Hopf bifurcation*

We now investigate Andronov-Hopf bifurcation. The first stage of this process involves determining the parameter likely to produce such a bifurcation.

The two slow-fast parameters  $\xi$  and  $\varepsilon$  cannot generate Hopf bifurcation because they leave invariant the fixed points, they cannot cancel the real part of the eigenvalues of the functional Jacobian matrix calculated for these points. It would also appear to be most useful to consider a parameter coupling the predator-prey and predator-top-predator equations.

The parameters  $\delta_1$  and  $\delta_2$  may be involved in bifurcation. The parameter  $\delta_1$  has the advantage of leaving invariant the  $x$ -co-ordinate and the  $y$ -co-ordinate of the singular point. The value of the bifurcation parameter can be calculated numerically as described in Sec. 2.3.11.

Thus, a Hopf bifurcation occurs:

- If the real part of the conjugated complex eigenvalues of the functional Jacobian matrix is cancelled for a certain value  $\delta_1 = \delta_{1C}$
- If the derivative with respect to  $\delta_1$  of this eigenvalue calculated in  $\delta_{1C}$  is non-zero
- If the other real eigenvalue evaluated in  $\delta_1$  is strictly negative.

The corresponding value of  $\delta_1$  is calculated as follows:

$$\text{Re}[\lambda_2] = 0$$

The numerical solution of this polynomial equation gives the following value:

$$\delta_1 = 0.683539$$

As the other two conditions are fulfilled, Hopf bifurcation occurs at

$$\delta_1 = 0.683539$$

Note:

The Routh & Hurwitz theorem can also be used to determine the value of the parameter  $\delta_1$  at which Hopf bifurcation occurs.

Indeed, by clarifying the characteristic polynomial of the Jacobian matrix at point J, we obtain a polynomial of the form:  $a_0 + a_1 \lambda + a_2 \lambda^2 + a_3 \lambda^3 = 0$ .

However, according to the Routh and Hurwitz theorem, all the roots of this polynomial have negative real parts when the determinants  $D_1$ ,  $D_2$  and  $D_3$  are all positive.

The positivity of the first determinant  $D_1$  fulfills a condition for  $\delta_1$  making it possible to obtain the value cited above ( $\approx 0.68$ ).

## 3.2. The Hastings-Powell model

By changing the variables followed in the Rosenzweig-MacArthur [1963] model, we can obtain the Hastings and Powell [1991] model

$$\begin{aligned}\frac{dx}{dt} &= a \left(1 - \frac{\lambda}{a} x\right) x - \frac{bxy}{H_1 + x} = xg(x) - byp(x) \\ \frac{dy}{dt} &= y \left( \frac{dx}{H_1 + x} - c \right) - \frac{eyz}{H_2 + y} = y[-c + dp(x)] - ezyq(y) \\ \frac{dz}{dt} &= z \left( \frac{fy}{H_2 + y} - g \right) = z[-g + fq(y)]\end{aligned}$$

### 3.2.1. Dimensionless equations

With the following changes of variables and parameters,

$$t \rightarrow \frac{1}{a} t, \quad x \rightarrow \frac{a}{\lambda} x, \quad y \rightarrow \frac{ad}{\lambda b} y, \quad z \rightarrow \frac{fba^2}{de\lambda} z$$

$$\begin{aligned}\frac{dx}{dt} &= x(1-x) - \frac{a_1 xy}{1 + \beta_1 x} \\ \frac{dy}{dt} &= y \left( \frac{a_1 x}{1 + \beta_1 x} - \delta_1 \right) - \frac{a_2 yz}{1 + \beta_2 y} \quad (28) \\ \frac{dz}{dt} &= z \left( \frac{a_2 y}{1 + \beta_2 y} - \delta_2 \right)\end{aligned}$$

with

$$a_1 = \frac{d}{\lambda H_1}, \quad \beta_1 = \frac{a}{\lambda H_1}, \quad a_2 = \frac{bf}{d\lambda H_2}, \quad \beta_2 = \frac{ad}{b\lambda H_2}, \quad \delta_1 = \frac{c}{a}, \quad \delta_2 = \frac{g}{a}$$

By choosing a set of "biologically reasonable" parameters, system (28) becomes a singularly perturbed system of two time scales.

### 3.2.2. Dynamic aspects

The natural time scale of the interaction between the predator  $y$  and the super-predator  $z$ , (i.e., of interaction at the higher trophic levels), is substantially longer than that between the prey  $x$  and the predator  $y$ . In other words,  $\delta_1$  is much larger than  $\delta_2$ .

Based the works of Ramdani *et al.* [2000], we consider the system (28) to be a slow-fast autonomous dynamic system for which we can determinate the equation of the slow manifold on which the attractor lies. A state equation binding the three variables can also be established established.

### *Nature and stability of the fixed points*

For the initial set of values used in this simulation ( $\xi = 1, \beta_1 = 3, \beta_2 = 2, \delta_1 = 0.4, \delta_2 = 0.01, \varepsilon = 1$ ) we obtain four equilibrium points (of biological significance) with the following eigenvalues:

$$O(0, 0, 0) \rightarrow \{1, -0.4, -0.01\}$$

$$I(0.1052, 0.2354, 0) \rightarrow \{0.00600753, 0.0547368 + 0.518656 i, 0.0547368 - 0.518656 i\}$$

$$J(0.8192, 0.125, 9.8082) \rightarrow \{-0.61121, 0.038687 + 0.0748173 i, 0.038687 - 0.0748173 i\},$$

$$K(1, 0, 0) \rightarrow \{-1, 0.85, -0.01\}$$

So according to the Lyapunov criterion, all these points are unstable.

The literal expression of the fixed points highlights their dependance on the parameters considered.

This finding will be used below, in the calculation of Hopf bifurcation.

### *Phase portrait*

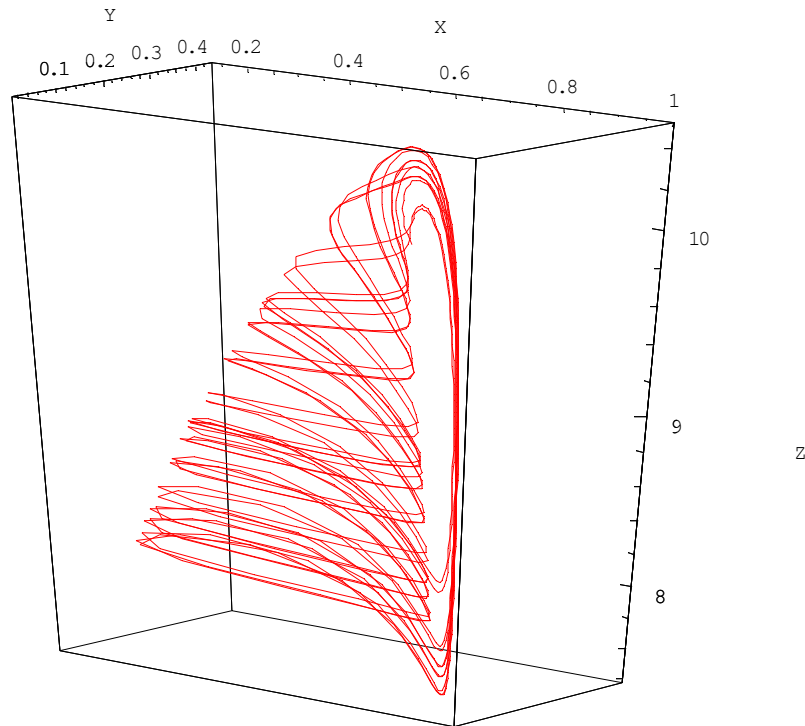


Fig. 7. Phase portrait of the Hastings and Powell system (28) with the same parameter values.

### 3.2.3. Slow manifold equation

#### Slow manifold equation based on the orthogonality principle

As describe in Sec. 2.4., the equation of the slow manifold can be expressed as follows:

$$\lambda_1 (\mathbf{x}, \mathbf{y}, \mathbf{z}) \mathbf{z}_{\lambda_1} (1, \beta (\mathbf{x}, \mathbf{y}, \mathbf{z}), \gamma (\mathbf{x}, \mathbf{y}, \mathbf{z}))$$

Let us call  $\lambda_1(x, y, z)$  the fast eigenvalue of  $\mathcal{J}(x, y, z)$  and  $\mathbf{z}_{\lambda_1}(1, \beta(x, y, z), \gamma(x, y, z))$  the fast eigenvectors to the left of  $\mathcal{J}(x, y, z)$ . Transposing the characteristic equation,

$${}^t (\mathcal{J} (\mathbf{x}, \mathbf{y}, \mathbf{z})) \mathbf{z}_{\lambda_1} (\mathbf{x}, \mathbf{y}, \mathbf{z}) = \lambda_1 (\mathbf{x}, \mathbf{y}, \mathbf{z}) \mathbf{z}_{\lambda_1} (\mathbf{x}, \mathbf{y}, \mathbf{z})$$

we can find  $\beta$  and  $\gamma$ .

$$\beta = \left( \frac{(1 + \mathbf{x}\beta_1)^2}{5\mathbf{y}} \right) \left( \lambda_1 - (1 - 2\mathbf{x}) + \frac{5\mathbf{y}}{(1 + \mathbf{x}\beta_1)^2} \right)$$

$$\gamma = \beta \frac{0.1\mathbf{y}}{0.1\mathbf{y} - (1 + \mathbf{y}\beta_2) (\delta_2 + \lambda_1)}$$

The slow manifold equation is thus given by:

$$\dot{\mathbf{x}} + \beta (\mathbf{x}, \mathbf{y}, \mathbf{z}) \dot{\mathbf{y}} + \gamma (\mathbf{x}, \mathbf{y}, \mathbf{z}) \dot{\mathbf{z}} = 0 \quad (29)$$

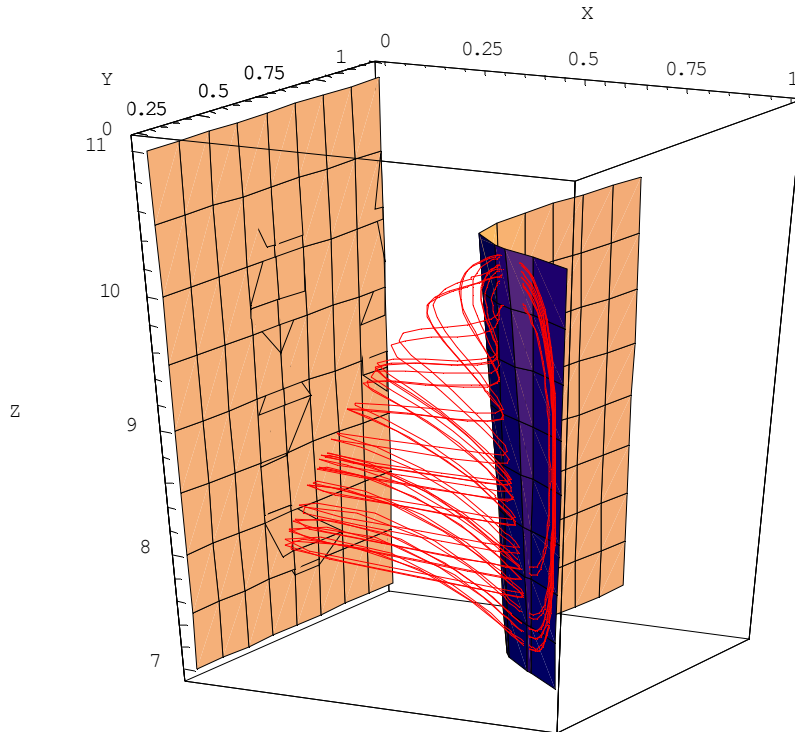


Fig. 8. Slow manifold surface based on the orthogonality principle and phase portrait of the Hastings and Powell system (28) with the same parameter values.

### 3.2.4. Hopf bifurcation

We will now focus on Andronov-Hopf bifurcation. The first stage in this process involves identifying the parameter likely to produce such a bifurcation.

The slow-fast parameters  $\xi$  and  $\varepsilon$  cannot generate bifurcation as they leave the fixed points invariant and they cannot cancel the real part of the eigenvalues of the functional Jacobian matrix calculated for these points. It would also be useful to consider a parameter coupling the two predator-prey and predator- top-predator equations.

The parameters  $\delta_1$  and  $\delta_2$  may also be considered. The parameter  $\delta_1$  has the advantage of leaving invariant the  $x$ -co-ordinate and the  $y$ -co-ordinate of the singular point. It also modifies the topology of the attractor, conferring on it the Moebius strip shape of the Rosenzweig-MacArthur model at a certain value .

We can therefore fix all the values of the parameters at the levels described above, except for  $\delta_1$ . The technique described in Sec. 2.3.11. can then be used for numerical calculation of the bifurcation parameter value.

Thus, Hopf bifurcation occurs:

- If the real part of the complex conjugated eigenvalues of the functional Jacobian matrix is cancelled for a certain value  $\delta_1 = \delta_{1C}$
- If the derivative with respect to  $\delta_1$  of this eigenvalue calculated in  $\delta_{1C}$  is non-zero
- If the other real eigenvalue evaluated in  $\delta_1$  is strictly negative.

The corresponding value of  $\delta_1$  is calculated as follows:

$$\text{Re}[\lambda_2] = 0$$

The numerical solution of this polynomial equation gives the following value:

$$\delta_1 = 0.7402$$

As the other two conditions are fulfilled, the Hopf bifurcation occurs at

$$\delta_1 = 0.7402$$

In addition, by selecting  $\beta_1$  as the bifurcation parameter and proceeding as describe above, it is possible to calculate the value of this parameter with a high degree of precision. Indeed, cancelling the part of the complex eigenvalues of the functional jacobian matrix evaluated at the fixed point I according to the parameter  $\beta_1$  generates the value:  $\beta_1 = 2.11379$ .

### 3.3. Similarity between the various models

#### 3.3.1. *Volterra-Gause and Rosenzweig-MacArthur*

The Volterra-Gause model, as described above, directly resembles the Rosenzweig-MacArthur model for certain parameter values.

Indeed, these two models present similar dynamic behaviour (Fig. 9). Below the bifurcation threshold, we find the overall shape of the chaotic attractor of the Rosenzweig-MacArthur model.

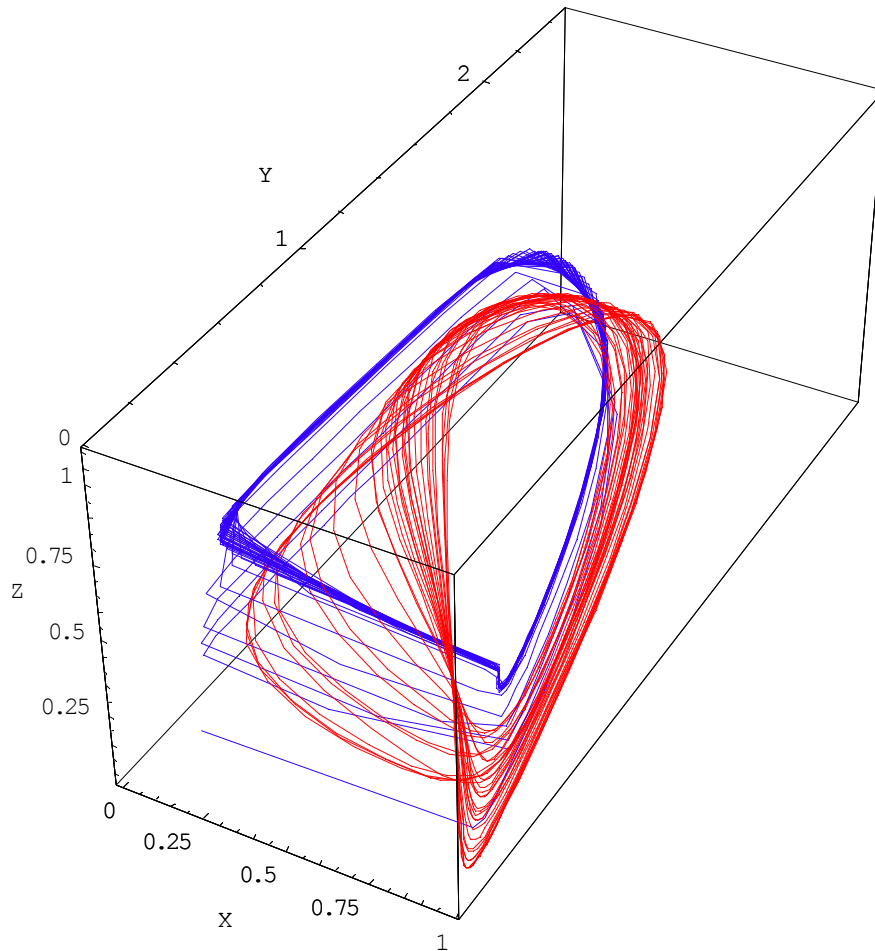


Fig. 9. Comparison of the Volterra-Gause model (for  $\xi = 0.964$ ,  $\varepsilon = 1.1$ ,  $\delta_1 = 0.518$ ,  $\delta_2 = 0.415$ ) and the Rosenzweig-MacArthur model (for  $\xi = 0.1$ ,  $\beta_1 = 0.3$ ,  $\beta_2 = 0.1$ ,  $\delta_1 = 0.1$ ,  $\delta_2 = 0.62$ ,  $\varepsilon = 0.3$ )

### 3.3.2. The Volterra-Gause and Hastings-Powell models

The similarity between the Volterra-Gause model and the Hastings and Powell model, with its famous "up-side-down teacup" is more striking. The following figures show the basic teacup shape and the behaviour of each component  $x, y, z$  over time.

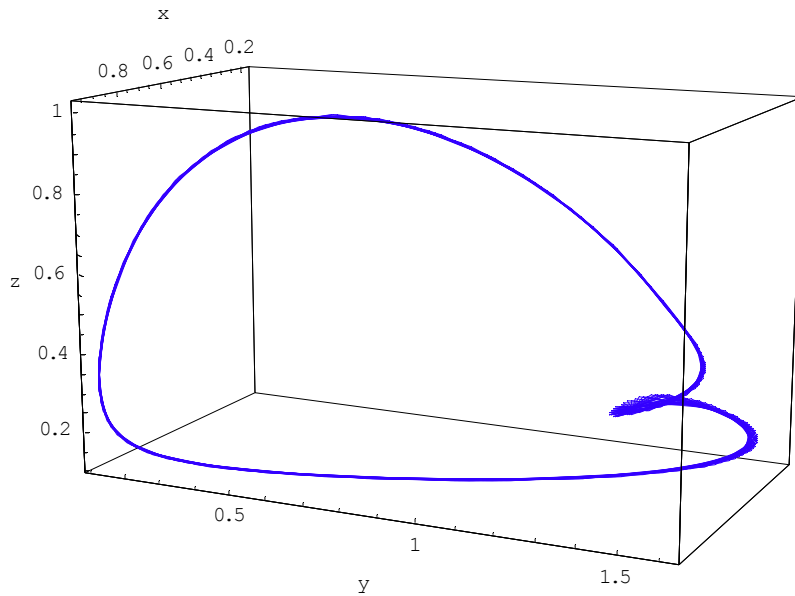


Fig. 10. Phase portrait of the Volterra-Gause model (for  $\xi = 0.07$ ,  $\varepsilon = 0.85$ ,  $\delta_1 = 0.5$ ,  $\delta_2 = 0.42$ )

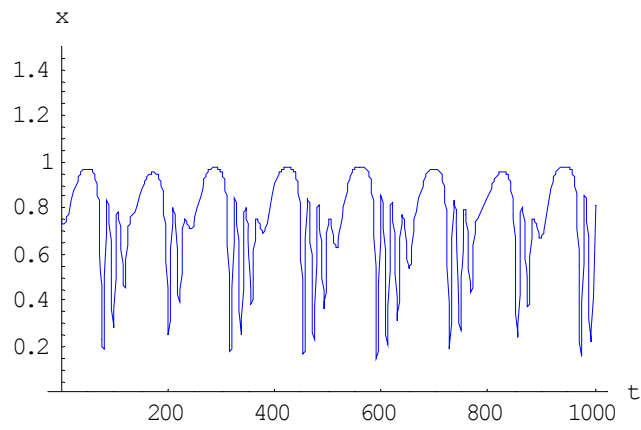
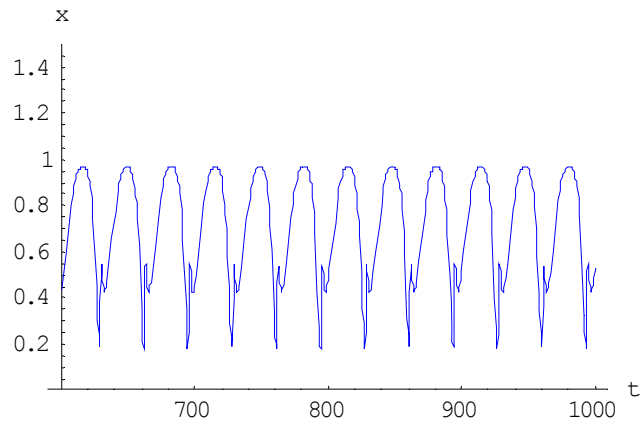


Fig. 11. Comparison of the changes over time in the Volterra-Gause (for  $\xi = 0.07$ ,  $\varepsilon = 0.85$ ,  $\delta_1 = 0.5$ ,  $\delta_2 = 0.42$ ) and Hastings-Powell models (for  $\xi = 1$ ,  $\beta_1 = 3$ ,  $\beta_2 = 2$ ,  $\delta_1 = 0.4$ ,  $\delta_2 = 0.01$ ,  $\varepsilon = 1$ ).

### 3.3.3. The Rosenzweig-MacArthur and Hastings-Powell models

The bifurcation parameter  $\delta_1$  chosen in Sec. 2.1.5. modifies the topology of the attractor of the Rosenzweig-MacArthur model conferring on it, at a certain value, the shape of the so-called "up-side-down tea-cup" of the Hastings and Powell [1991] model.

We can therefore fix all the parameters at values cited above, except for  $\delta_1$ . Varying the parameter  $\delta_1$  up to a value of 0.3, preserves a limit cycle, which becomes deformed, resulting in a passage from the Rosenzweig-MacArthur model to the Hastings and Powell model.

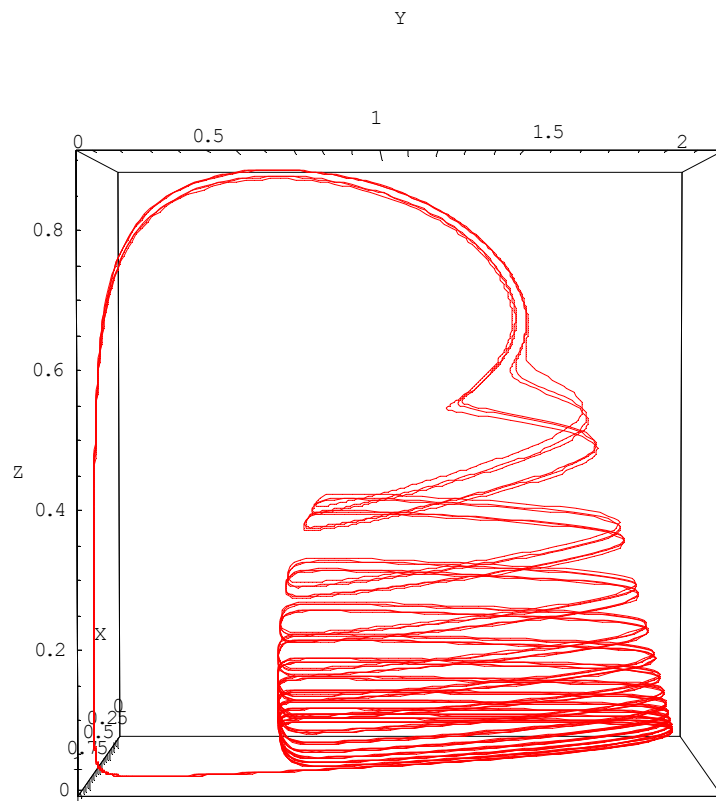


Fig. 12. Transition from the Rosenzweig-MacArthur model to the Hastings and Powell [1991] model

In this figure, we can identify the attractor in the shape of a teacup, for the Hastings and Powell [1991] model with  $\delta_1 = 0.3$ .

### 3.3.4. *The Hastings-Powell and Rosenzweig-MacArthur*

The Hastings-Powell model can also be converted to the Rosenzweig-MacArthur model.. Varying the bifurcation parameter  $\delta_1$  modifies the topology of the attractor, conferring on it the Moebius strip shape of the Rosenzweig-MacArthur model at a certain value.

We can therefore fix all the parameters at the values cited above, except for  $\delta_1$ .

Variation of the parameter  $\delta_1$  up to a value of 0.1, results in a passage from the model of Hastings and Powell to the of Rosenzweig-MacArthur model.

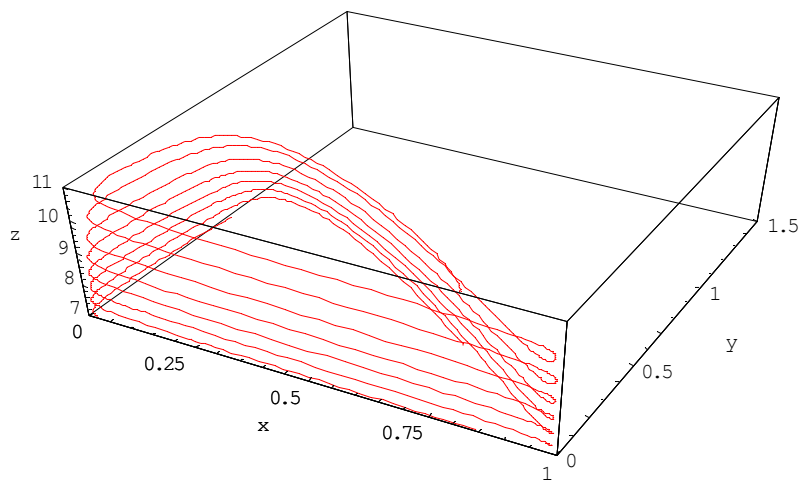


Fig. 13. Transition from the Hastings and Powell model to Rosenzweig-MacArthur model. On this figure, we can see the attractor with the Moebius strip shape of Rosenzweig-MacArthur model at  $\delta_1 = 0.1$ .

## 4. Discussion

In this work, we have shown certain similarities between the three models considered. The common features of these models, the possibility of transition from one model to another by parameter variation and the differences between these models provide biologists with alternatives in their choice of predator-prey model. Despite differences in their functional responses, these models present striking similarities in the nature and number of their fixed points, and in their dynamic behaviour: existence of a limit cycle, occurrence of Hopf bifurcation, presence of a chaotic attractor or period doubling cascades.

Dynamical features \ Models	Rosenzweig – Mac Arthur		Hastings – Powell		Volterra – Gause	
	$O(0, 0, 0)$ $J(x^*, y^*, z^*)$	$I(\hat{x}, \hat{y}, 0)$ $K(1, 0, 0)$	$O(0, 0, 0)$ $J(x^*, y^*, z^*)$	$I(\hat{x}, \hat{y}, 0)$ $K(1, 0, 0)$	$O(0, 0, 0)$ $J(x^*, y^*, z^*)$	$I(\hat{x}, \hat{y}, 0)$ $K(1, 0, 0)$
Attractional sink	2		2		2	
Hopf bifurcation	$\delta_1 = 0.6835$		$\delta_1 = 0.7402$		$\delta_1 = 0.7474$	
Chaotic attractor	Moebius strip		Tea cup		Snail shell	
Period – doubling	$\delta_2 = 0.67785$		$b_1 = 2.437$		$\delta_1 = 0.625$	
Slow manifold	1		1		1	

The fixed point  $O(0, 0, 0)$  presents the same stability in all three models, with attractive eigendirections according to  $z'z$  and repulsive eigendirections according to  $x'x$ . The eigendirections of point  $K(1, 0, 0)$  are attractive according to  $x'x$  and  $z'z$  in all three models. Points  $I(\hat{x}, \hat{y}, 0)$  and  $J(x^*, y^*, z^*)$  behave as a stable and an unstable focus, respectively, with  $I$  in the  $xy$  plane and  $J$  apart from the  $xy$  plane. These models introduce rich and complex dynamics, for which further study is required.

It also appears to be possible, in some domains of parameter variation, to reduce the dimension of the models, making it possible to take into account the influence of the external medium by means of time-dependent coefficients.

## Acknowledgements

Certain numerical results and graphs were not possible without the use of powerful programs designed by Eric Javoy.

---

## References

- Deng, B. [2001] "Food chain chaos due to junction-fold point," *Am. Inst. of Physics* **11** (3), 514-525.
- Freedman, H.I. & Waltman, P. [1977] "Mathematical analysis of some three-species food-chain models," *Mathematical Biosciences* **33**, 257-276.
- Gause, G.F. [1935] *The struggle for existence* (Williams and Wilkins, Baltimore)
- Glass, L. & Mackey, M.M. [1988] *From clocks to chaos* (Princeton University Press, Princeton, New Jersey, USA).
- Hastings, A. & Powell, T. [1991] "Chaos in a three-species food chain," *Ecology* **72**, 896-903.
- Holling, C.S. [1959] "Some characteristics of simple types of predation and parasitism," *Can. Entomologist* **91**, 385-398.
- Kuznetsov, Y. [1995] *Elements of Applied Bifurcation Theory* (Springer & Verlag, New York).
- Lotka, A.J. [1925] *Elements of Physical Biology* (Williams and Wilkins, Baltimore).
- Muratori, S. & Rinaldi, S. [1992] "Low and high frequency oscillations in three dimensional food chain systems," *SIAM J. Appl. Math.* **52**, 1688-1706.
- Ramdani, S., Rossetto, B., Chua, L. & Lozi R. [2000] "Slow Manifold of Some Chaotic Systems-Laser Systems Applications," *Int. J. Bifurcations and Chaos* **10**, Vol.12, 2729-2744.
- Rinaldi, S. & Muratori, S. [1992] "Slow-fast limit cycles in predator-prey models," *Ecological Modelling* **61**, 287-308.
- Rosenzweig, M.L. & Mac Arthur, R.H. [1963] "Graphical representation and stability conditions of predator-prey interactions," *Am. Nat.* **97**, 209-223.
- Rosenzweig, M.L. [1971] "Paradox of enrichment : destabilisation of exploitation ecosystems in ecological time," *Science* **171**, 385-387.
- Verhulst, P.F. [1838] "Notice sur la loi que suit la population dans son accroissement," *Corresp. Math. Phys.* **X**, 113-121 [in French].
- Volterra, V. [1926] "Variazioni e fluttuazioni del numero d'individui in specie animali conviventi," *Mem. Acad. Lincei* III **6**, 31-113 [in Italian].